Journal of Neuroscience Methods 194 (2011) 380–385

Contents lists available at ScienceDirect

Journal of Neuroscience Methods

journal homepage: www.elsevier.com/locate/jneumeth

Application of multidimensional scaling to quantify shape in Alzheimer's disease and its correlation with Mini Mental State Examination: A feasibility study☆

Hyunjin Park[a], Jongbum Seo[b,*], the ADNI[1]

[a] Dept. of Biomedical Eng., Gachon Univ. of Medicine and Science, Incheon, South Korea
[b] Dept. of Biomedical Eng., Yonsei University, Wonju, South Korea

ARTICLE INFO

Article history:
Received 18 May 2010
Received in revised form
29 September 2010
Accepted 20 October 2010

Keywords:
Shape
Multidimensional scaling
Alzheimer's disease
Mini Mental State Exam
Image registration

ABSTRACT

Today, high-resolution MRI scans are able to reveal even the fine details of brain structure. Several methods have been developed to quantify shape differences specific to scans of diseased brains. We have developed a novel method for quantifying shape information based on multidimensional scaling (MDS), a well-known statistical tool. Multidimensional scaling uses distance measures computed from pair-wise image registration of the training set. Image registration establishes spatial correspondence between scans in order to compare them in the same spatial framework. Our novel method has several advantages, including robustness to errors in registrations. Applying our method to 44 brain MRIs showed clear separation between normal and Alzheimer scans. Using our method as basis for classification between normal and Alzheimer scans yielded better performance results compared with using the volume of hippocampus as basis for classification. We also devised a simple measure derived from the MDS approach that was shown to correlate with the Mini Mental State Examination (MMSE), a well-known cognitive test for Alzheimer's disease.

1. Introduction

It is now possible to study the brain anatomy of a specific population with high-resolution scans of a wide range of patients. In the neuroimaging realm, researchers have used high resolution (around 1 mm) T1-weighted MRI scans to study brain structures hypothesized to be affected by disease. Image analysis techniques, such as a simple volume measurement or a complex shape measurement, are applied to structures of interest in order to quantify changes that may relate to a specific disease process. Researchers have developed computer algorithms to model those changes. The scope of these projects has rapidly expanded in recent years, and they have been grouped into a discipline referred to as computational anatomy (Grenander and Miller, 1998; Ashburner et al., 2003).

Some neurodegenerative diseases cause distinct morphological changes in the brain's gross anatomy. For example, Alzheimer's disease typically results in atrophy in the hippocampal region. Computer algorithms that detect such morphological changes (i.e., a smaller hippocampus with respect to those of a normal control group) represent a clinical application of computational anatomy. The ability of a computer algorithm to detect morphological signatures specific to a disease has the potential to improve diagnosis and treatment of a variety of neurodegenerative diseases. In this paper, we focus on Alzheimer's disease (AD).

Computational anatomy studies the morphology of a specific population. The measurement of shape is a complex topic and has been a matter of significant controversy (Ashburner and Friston, 2001; Friston and Ashburner, 2004; Bookstein, 2001; Davatzikos, 2004). There are two major approaches described in the literature. The first approach, called deformation-based morphometry (DBM), assumes that all shape information is encoded into the deformation fields associated with different scans in the population (Ashburner et al., 1998; Thompson and Toga, 1999). Deformation fields are computed by registering two scans non-linearly, i.e., identifying the best geometric transform between them. The second approach, called voxel-based morphometry (VBM), assumes that all shape information is encoded in some scalar function of spatially normalized scans (Ashburner and Friston, 2000). For example, two scans are segmented (i.e., labeled) and then linearly registered so that both scans are in the same spatial coordinates. After registration,

☆ Data used in the preparation of this article were obtained from the Alzheimer's Disease Neuroimaging Initiative (ADNI) database (www.loni.ucla.edu/ADNI). As such, the investigators within the ADNI contributed to the design and implementation of ADNI and/or provided data but did not participate in analysis or writing of this report. ADNI investigators include (complete listing available at http://www.loni.ucla.edu/ADNI/Collaboration/ADNI_Manuscript_Citations.pdf).

* Corresponding author. Tel.: +82 33 760 2478; fax: +82 33 765 5483.
E-mail addresses: hyunjinp@gachon.ac.kr (H. Park), jongbums@yonsei.ac.kr, hyunjinp@gmail.com (J. Seo).

[1] The Alzheimer's Disease Neuroimaging Initiative.

0165-0270/$ – see front matter © 2010 Elsevier B.V. All rights reserved.
doi:10.1016/j.jneumeth.2010.10.019

the shape information is assessed using voxel-wise differences in the labels.

DBM uses deformation fields obtained from registrations of scans of a population and identifies differences in the relative positions of structures within organs. Analysis of the deformation field needs to remove the confounding effects caused by varying positions and sizes of the structure of interests. Procrustes shape analysis removes much of these confounding effects (Bookstein, 1997). The biggest shortcoming of DBM is that it requires a very accurate registration algorithm to compute the displacement field, as the process is solely based on the displacement field. Registration is computed by either a set of manually identified landmarks or a very high degrees of freedom (DOF) registration algorithm (Bookstein, 1997). A perfect non-linear registration between scans results in all of the information needed to assess shape changes between scans. DBM is a solid platform for evaluating shape information that requires precise computation of displacement fields.

We assume that the shape information is coming from the deformation fields given very accurate registrations. We propose to make DBM more robust to imperfect registrations. Our DBM-based approach improves robustness with respect to imperfect registrations using a well-known statistical framework called multidimensional scaling (MDS). We applied our MDS-based shape quantification method to separate patients with AD from the aged-matched normal controls. We also devised a simple measure from the MDS approach and showed that it was meaningfully correlated with the Mini Mental State Examination (MMSE), a well-known cognitive test commonly used to assess AD many forms of dementia including AD.

2. Materials and methods

MDS is a technique for producing relative positional locations from a collection of pair-wise distances. Our MDS-based method has two components to improve the robustness with respect to imperfect registrations. First, we compress the entire deformation field, whose DOFs are on the order of the number of voxels, to the single scalar value noted as distance. The effects of imperfect registrations will be less evident using the single scalar value than those using the deformation field. Second, we conduct multiple measurements of the single scalar value (i.e., distance) between various configurations in order to improve the sensitivity to shape change. For example, for N scans, instead of computing $N-1$ deformation fields and distances with respect to a chosen target scan, we compute deformation fields and distances with respect to all possible pairs of target and source scans (i.e., N choose $2 = N(N-1)/2$ scans). Multiple distance measurements correspond to pair-wise distances in the MDS framework. In summary, we compress the deformation into a single scalar value (distance) to improve robustness to mis-registrations and perform multiple measurements at different configurations to improve the sensitivity to shape change.

2.1. Registration framework

Registration is a task of mapping one image onto another. Registration is central to DBM, as it computes displacement fields that will be analyzed as shape information. Registration itself has been discussed extensively in the literature (Pluim et al., 2003; Hill et al., 2001). In short, two main components must be determined for any registration method: the similarity measure which measures the degree of alignment between images and the geometric interpolant which defines the geometric transform. This study used mutual information (MI) as the similarity measure and thin-plate splines (TPS) as the geometric interpolant (Bookstein, 1989). We implemented the registration software as described in Meyer et al. (1997).

2.2. Distance measure

Registration between two images yields a geometric transform optimized to maximize a certain cost function, such as MI. The displacement field is a collection of evaluations of the geometric transform at all voxel locations. We compressed the entire deformation field, whose order is equal to the number of voxels, to a single scalar value (distance). The geometric distance, hereafter called distance, between two scans is usually measured by the roughness of the geometric transform that associates the coordinate spaces of two images. However, we preferred the distance to have invariance to affine transforms. Roughness of the geometric transform can be measured by integrating the squared value of nth-order partial derivatives of the transform. Second-order derivatives are chosen to ensure invariance to affine transforms. We define the distance between two scans as the sum of the squared second-order partial derivatives of the geometric transform.

$$d^2 = \int\int \left(\frac{\partial^2 f_x}{\partial x^2}\right)^2 + 2\left(\frac{\partial^2 f_x}{\partial x \partial y}\right)^2 + \left(\frac{\partial^2 f_x}{\partial y^2}\right)^2 dx\,dy + \int\int \left(\frac{\partial^2 f_y}{\partial x^2}\right)^2 + \left(\frac{\partial^2 f_y}{\partial x \partial y}\right) 2^2 + \left(\frac{\partial^2 f_y}{\partial y^2}\right)^2 dx\,dy \quad (1)$$

f_x; displacement in x f_y; displacement in y.

Formulation in (1) is for two dimensions, but it can be easily extended for 3D. The distance calculated using this equation is often called the bending energy. Analytic formulae for calculating bending energy are available for TPS (Bookstein, 1989). For other geometric transforms, the bending energy may need to be calculated numerically. The defined distance is not strictly a metric since the distance between two different images can be zero if both images can be registered using an affine transform.

2.3. Multidimensional scaling (MDS)

MDS is a technique for producing relative positional locations from a collection of pair-wise distances (Torgerson, 1952; Young and Hamer, 1994). The relative locations are accurate up to an arbitrary rotate-translate transform. For example, $N(N-1)/2$ (i.e., N choose 2) pair-wise distances are needed to apply MDS to visualize the relative locations of N cities. The distances used in MDS need not be metric, as non-metric distances such as ranking can be used. Therefore, the distance we defined in the previous subsection can be used in MDS settings. Given a set of distances in the distance matrix D, where d_{ij} refers to the distance between objects i and j, MDS outputs a set of coordinates in a user-specified dimension that best reproduces the distance matrix in the least-square fashion. The dimension of MDS output is determined based on the eigenstructure of the distance matrix. The output coordinates are in the standard Euclidean space of the user-chosen dimension.

2.4. Shape quantification based on MDS

We intend to improve the DBM-based shape quantification method. First, the whole deformation field is compressed to a single scalar value (distance). Second, we conduct multiple measurements of the distance at various configurations in order to improve the sensitivity to shape change. For example, for N scans, instead of computing $N-1$ deformation fields and distances with respect to a chosen target scan, as is typically done in DBM, we compute N choose 2 (i.e., $N(N-1)/2$) deformation fields and distances

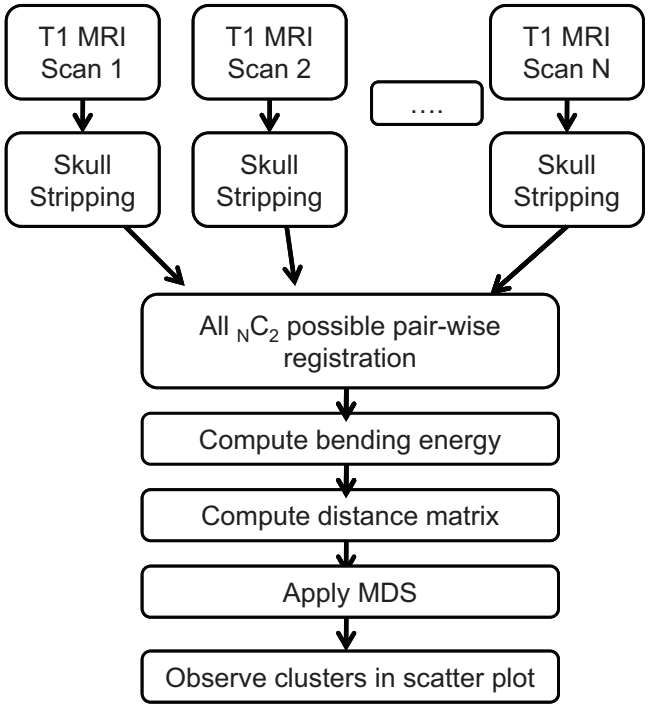

Fig. 1. Shape quantification procedures using MDS for *N* scans.

with respect to all possible combination of target and source scans. Multiple distance measurements correspond to pair-wise distances in the MDS framework. Our approach fits the MDS framework well since MDS measures all possible pair-wise distances. MDS outputs a collection of high-dimensional coordinates in Euclidean space, each of which represents an object: in this case, a scan. With MDS, we can compute the relative positions of all scans in the Euclidean space of a user-chosen dimension. We hypothesize that scans of the same type, either normal or abnormal, will be placed adjacent and scans of different types will be placed separately. Therefore, we hypothesize that MDS results will lead to a scatter plot in which two distinct clusters can be observed. In summary, we hypothesize that using MDS with pair-wise distances based on registrations will provide a framework for shape quantification. Fig. 1 is the procedure for *N* scans.

2.5. Scan acquisition

We obtained MRI image data and the associated cognitive test results (including MMSE scores) from the Alzheimer's Disease Neuroimaging Initiative (ADNI) database. Following is a brief description of the ADNI effort. Data used in the preparation of this article were obtained from the Alzheimer's Disease Neuroimaging Initiative (ADNI) database (www.loni.ucla.edu/ADNI). The ADNI was launched in 2003 by the National Institute on Aging (NIA), the National Institute of Biomedical Imaging and Bioengineering (NIBIB), the Food and Drug Administration (FDA), private pharmaceutical companies and non-profit organizations, as a $60 million, 5-year public–private partnership. The primary goal of ADNI has been to test whether serial magnetic resonance imaging (MRI), positron emission tomography (PET), other biological markers, and clinical and neuropsychological assessment can be combined to measure the progression of mild cognitive impairment (MCI) and early Alzheimer's disease (AD). Determination of sensitive and specific markers of very early AD progression is intended to aid researchers and clinicians to develop new treatments and monitor their effectiveness, as well as lessen the time and cost of clinical trials. We acquired 44 MRI brain scans and noted the MMSE score for each patient. Nine scans were identified with Alzheimer's disease, and nine scans were identified as age-matched normal controls. AD scans were of patients aged 67.5–82.2 years (median 72.7). Normal scans were of patients aged 70.8–89.7 years (median 78.7). All MRIs were sagittal T1-weighted scans and had typical dimensions of $256 \times 256 \times 166$ and resolutions of $0.94\,\text{mm} \times 0.94\,\text{mm} \times 1.2\,\text{mm}$. The scans were collected using a 1.5T GE Signa scanner with MP-RAGE acquisition sequence.

2.6. Data pre-processing

We removed non-brain tissues from all 44 scans using a procedure called "skull stripping", for which many algorithms are readily available (Bedell and Narayana, 1998). In our procedure, we applied our own skull stripping algorithm based on registration. First, registration between the labeled International Consortium for Brain Mapping (ICBM) scan and the user-chosen scan was established. Second, labels from the ICBM scan were carried onto the user scan and then used as a mask. Masked voxels contained only brain tissues including white matter, gray matter, and cerebral spinal fluid (CSF). With this mask, the user-chosen scan could be stripped of non-brain tissues. The accuracy of this method depends on the

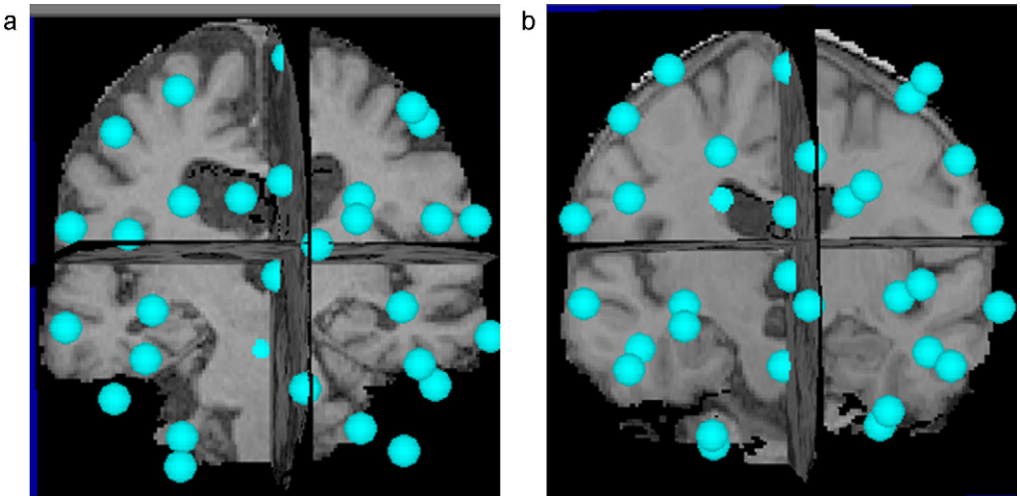

Fig. 2. Sample brain MRI scans. Samples of the skull stripped brain scans with control points are given. The left figure is AD and the right figure is normal control. Control points are given in blue dots. (For interpretation of the references to colour in this figure legend, the reader is referred to the web version of this article.)

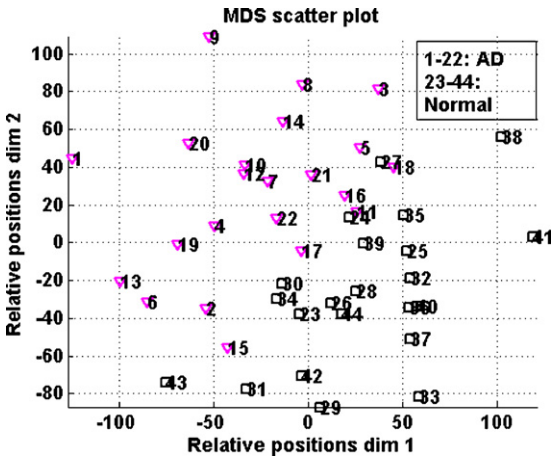

Fig. 3. Output of three-dimensional MDS. Only the first two of three dimensions were plotted due to space constraints. Scans 1–22 are AD cases marked with magenta triangles. Scans 23–44 are normal control cases marked with black squares. Major separation occurred along the second dimension. (For interpretation of the references to colour in this figure legend, the reader is referred to the web version of this article.)

accuracy of the registration between the ICBM scan and the user-chosen scan. We used TPS-based registration with approximately 60 DOFs (i.e., 20 control points) to establish registration between the ICBM scan and the user-chosen scan.

After all scans were removed of non-brain tissues, pair-wise registrations using 50 control points were performed. The 50 control points were distributed almost uniformly over the entire brain. Typical samples of the skull stripped brain scans with control points are shown in Fig. 2. There were 946 (i.e., 44 choose 2) pair-wise registrations involved. Once all of the pair-wise registrations were completed, distance values (i.e., bending energies) were computed and entered into the distance matrix. The upper half of the matrix was computed, and the lower half was duplicated, thus a symmetric distance matrix was assumed.

3. Results

3.1. Results: testing separability between clusters

MATLAB (Mathworks Inc., Natick, MA, USA) was used to compute the statistical results in Section 3. After the distance matrix was computed, MDS was applied and the results were analyzed in three dimensions. The dimensionality of MDS was chosen based on the eigenvalues of the distance matrix. Eigenvalues obtained from singular value decomposition (SVD) were plotted in a descending fashion; we chose the number L as the dimension, such that after L largest eigenvalues, the next occurring eigenvalue dropped dramatically. The output of MDS was plotted in Fig. 3. Each coordinate represents a scan from 44 training scans. As we had hypothesized, there were two distinct clusters for normal and abnormal scans. Scans 1–22 were of patients with AD, and scans 23–44 were of normal controls. The two clusters seemed to be separable along the second coordinate dimension (the vertical axis). A two-sample t-test on the second coordinates of the MDS output showed a p-value of 6×10^{-5}. Thus, the two clusters were likely to have different means. In summary, we showed the separability of two classes, normal and AD, with 44 MRI scans.

3.2. Results: classification between AD and normal

In this section, we compared classification performance between AD and normal based on our MDS approach and the established approach using hippocampus volume. The volume of hippocampus was reported to be a good feature to classify between AD and normal (Duchesne et al., 2008). Simply put, AD patients tend to have smaller hippocampus compared to normal controls. We used the well-known FSL software to automatically segment the hippocampus and computed its volume (Woolrich et al., 2009). Manual segmentation is better in terms of accurately segmenting the hippocampus but is very labor intensive so we chose the automatic segmentation method. For our MDS approach, we used the separable coordinates of MDS scatter plot to classify between AD and normal. We adopted k-nearest neighbor (kNN) classification algorithm for both approaches, where k is set to three. A leave-one-out approach was adopted when computing the classification performance. For each case being tested, we trained the classifier using the remaining 43 cases and then computed the classification performance for the test case. The process was repeated for all 44 cases and the classification rate was reported. Our MDS approached yielded 86.3% accuracy, while the approach based on hippocampus volume yielded 75.0% accuracy. Thus, we observed performance improvements of classification rate using the MDS coordinates over the use of hippocampus volume.

3.3. Robustness to mis-registrations

In this section, we present the simulation results regarding the robustness of MDS-based shape quantification. We performed two simulated trials. In the first trial, we added registration noise to one of the many pair-wise registrations and observed the p-value of the two sample t-tests on the second coordinates of the MDS output. A low p-value indicates that the two clusters have different means (i.e., are separable), and a high p-value indicates that the two clusters have the same mean (i.e., are not separable). p-Values were measured as we increased the magnitude of the added registration noise to one chosen pair-wise registration. Registration noise was implemented by randomly perturbing the optimized TPS control point location by a zero mean Gaussian of appropriate standard deviation.

For the first trial, we observed that the p-value did not change as we increased the magnitude (i.e., standard deviation) of the added registration noise, as shown in the left plot of Fig. 4. The p-value remained stable even at a standard deviation of 50 mm, where the size of the scan was 240 mm $\times$ 240 mm $\times$ 198 mm. This implies that one erroneous pair-wise registration out of 946 possible registrations does not affect the p-value. As long as only one pair-wise registration was affected, we witnessed a similar trend: a relatively constant p-value despite increased registration noise.

In the second trial, we fixed the amount of registration noise but increased the number of pair-wise registrations affected. The zero mean Gaussian noise of standard deviation 20 mm was added to optimized locations of TPS control points for randomly chosen pair-wise registrations. The p-values were measured as the number of affected pair-wise registration increased. The p-value stayed relatively constant initially, but eventually increased as more pair-wise registrations were affected. This is shown in the right plot of Fig. 4. The p-value with 60 (out of 946 possible registrations) erroneous registrations was fairly close to the p-value with no affected pair-wise registrations. This implies that our shape quantification is sufficiently robust to withstand many erroneous registrations.

3.4. MDS distance and Mini Mental State Examination (MMSE)

The MMSE is a well-known cognitive test to assess and follow AD (Apostolova et al., 2006). Typically, an MMSE score of 30 is normal, scores between 23 and 29 signify mild impairment, and scores below 23 signify possible dementia. Although it is not the most accurate test, it is widely used. In the remainder of this section,

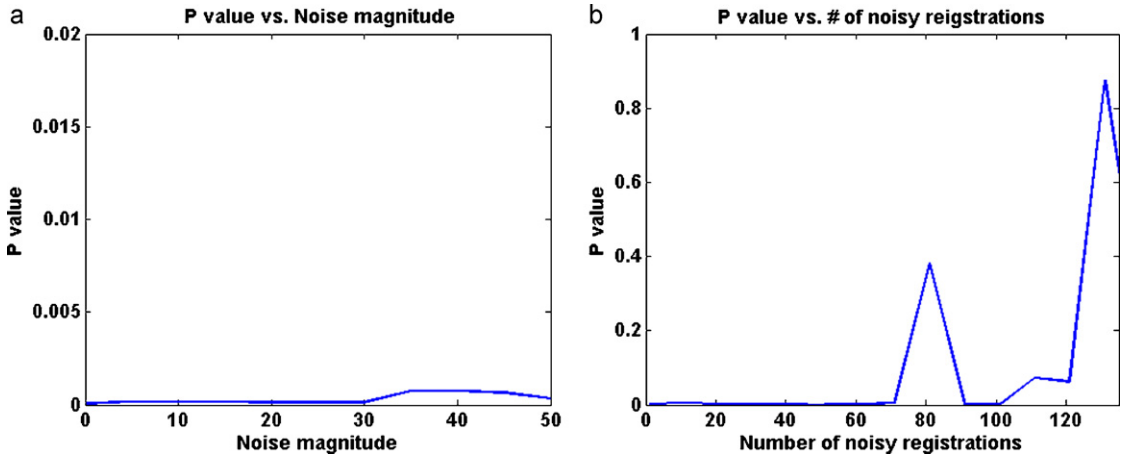

Fig. 4. Plot of *p*-value with respect to noisy registrations. The left plot is the *p*-value measured as the noise magnitude increases for one pair-wise registration. The right plot is the *p*-value measured as the number of affected pair-wise registration increases. The magnitude of registration noise is set at zero mean Gaussian with a standard deviation of 20 mm for the right plot.

we further demonstrate the effectiveness of our MDS approach. MDS provides relative locations for all scans, so the mean location of a group is easily defined. The mean location of the normal group is a simple sample mean of the MDS coordinate of the normal scans. Distance between scans may be computed by calculating the Euclidean distance (i.e., L2 norm) between the respective MDS coordinates. We hypothesize that, if an AD scan is far from the mean location of normal scans, then it will be associated with a low MMSE score. The rationale behind this hypothesis is that a severe AD scan is likely to be morphologically more different with respect to a normal scan than is a less severe AD scan. In MDS terms, this means that a severe AD scan will be further away from the mean of normal scans than will a less severe AD scan. Note that each patient had an MDS distance and a corresponding MMSE score. We plotted MDS distance and MMSE scores in Fig. 5. The MDS distance was computed as the Euclidean distance between an AD scan and the mean of the normal group. A negative correlation (i.e., as MDS distance increased, MMSE score decreased) was observed in nine AD samples. A correlation of −0.33 with a *p*-value of 0.13 was observed. Neglecting one outlier led to a correlation of −0.53 with a *p*-value of 0.01. Nonetheless, the negative correlation between MDS distance and MMSE score was notable. Note that MMSE scores themselves are subject to variability (Molloy and Standish, 1997). Patients with the same neuronal degeneration may have different MMSE scores if tested on different healthcare environments possibly due to differential quality of healthcare they receive. This variability in MMSE is another reason that a perfect linear relationship between MMSE scores and MDS distance was not possible. Increased variability in MMSE might lead to decrease in absolute value of the correlation (i.e., more dispersed dots in Fig. 5). We wanted to show correlation of MDS derived distances with easily obtainable clinical measures of cognitive impairment. MMSE was chosen since it was easily available not because it was the most accurate.

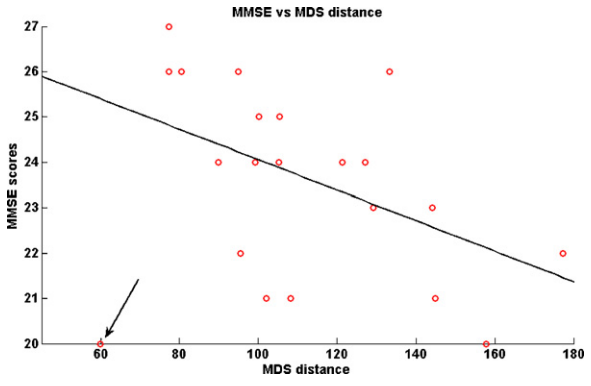

Fig. 5. Plot of MDS distance and MMSE score. A straight line with a negative slope is drawn for easer visualization. There are nine samples (red dots) in the plot. An outlier, indicated with an arrow, is observed in the lower left-hand corner. Most of the dots occur near the straight line. The regression equation is MMSE = −0.034 × MDS_distance + 27.4. (For interpretation of the references to colour in this figure legend, the reader is referred to the web version of this article.)

4. Discussions

The demonstration of separability between normal and AD scans combined with the correlation between MDS distance and MMSE scores will act as a good basis for designing a classification algorithm. This may ultimately contribute to improvements in computer-aided diagnosis (CAD) for AD. In the past, there have been efforts to use shape measurement over a volume of interest (VOI) (Duchesne et al., 2008) as a basis for CAD. In addition, some researchers have adopted normalized grayscale values of VOI as a basis for CAD (Duchesne et al., 2005). Defining VOI requires manual definition by an expert, which is time-consuming and subject to operator bias. The difficulties of defining VOI are circumvented using our MDS-based shape quantification as the basis for CAD, because the pair-wise distance (i.e., registration) of the MDS is performed over the entire volume. As demonstrated in Section 3.3, our approach is quite robust to errors in registration, which in turn leads to a robust basis for CAD.

Artificial intelligence based algorithms namely non-linear dimensionality reduction algorithms have been successfully applied to medical image analysis. In this paper, the observed data were the high-dimensional deformation fields whose dimensionality was reduced to the dimension of MDS. Recent advances in non-linear dimensionality reduction include kernel principal component analysis (Schölkopf et al., 1997), isomap (Roweis and Saul, 2000), diffusion map (Lafon, 2004), local MDS (Venna and Kaski, 2006), and manifold sculpting (Gashler et al., 2008). Our approach is similar to isomap and local MDS where pair-wise distances are extensively used.

We note that a more clinically relevant problem is to identify early stages of AD or mild cognitive impairment (MCI). Shape changes related to MCI are smaller in magnitude compared to the shape changes in AD with respect to normal control. In principle, the same MDS based approach may be applied to MCI versus nor-

mal scenario, which might lead to better separability between two groups than some of the existing methods. Some tweaks to handle the smaller shape differences must be incorporated. We leave this interesting problem as future work.

5. Summary

In summary, we have proposed an alternative to DBM-based shape quantification. Our algorithm is based on MDS, in which pair-wise distances are computed from pair-wise registrations. We have shown that our algorithm was able to detect differences between AD scans and normal scans using a 44-patient pilot study. We have also provided simulated results showing that the separability between clusters was maintained even in the case of noisy registrations, demonstrating the robustness of our shape quantification method. A simple MDS distance was meaningfully correlated with MMSE scores for AD patients, although the sample size of 44 is too small to draw statistical conclusions. Therefore, we plan to test our approach in the future using a larger sample size. Our study is a feasibility study to show that a well-established statistical tool, MDS, can be effective for shape quantification and CAD in AD.

Acknowledgements

This study was supported by 1) Basic Science Research Program through the National Research Foundation of Korea(NRF) funded by the Ministry of Education, Science and Technology (grant 20100023233), 2) Business for Cooperative R&D between Industry, Academy, and Research Institute funded Korea Small and Medium Business Administration in 2010 (grant 0850110), and 3) Ministry of Knowledge Economy of Korea (grant 10030091).

Data collection and sharing for this project was funded by the Alzheimer's Disease Neuroimaging Initiative (ADNI) (National Institutes of Health Grant U01 AG024904). ADNI is funded by the National Institute on Aging, the National Institute of Biomedical Imaging and Bioengineering, and through generous contributions from the following: Abbott, AstraZeneca AB, Bayer Schering Pharma AG, Bristol-Myers Squibb, Eisai Global Clinical Development, Elan Corporation, Genentech, GE Healthcare, GlaxoSmithKline, Innogenetics, Johnson and Johnson, Eli Lilly and Co., Medpace, Inc., Merck and Co., Inc., Novartis AG, Pfizer Inc., F. Hoffman-La Roche, Schering-Plough, Synarc, Inc., as well as non-profit partners the Alzheimer's Association and Alzheimer's Drug Discovery Foundation, with participation from the U.S. Food and Drug Administration. Private sector contributions to ADNI are facilitated by the Foundation for the National Institutes of Health (www.fnih.org). The grantee organization is the Northern California Institute for Research and Education, and the study is coordinated by the Alzheimer's Disease Cooperative Study at the University of California, San Diego. ADNI data are disseminated by the Laboratory for Neuro Imaging at the University of California, Los Angeles. This research was also supported by NIH Grants P30 AG010129, K01 AG030514, and the Dana Foundation.

References

Apostolova LG, Lu PH, Rogers S, Dutton RA, Hayashi KM, Toga AW, et al. 3D mapping of mini-mental state examination performance in clinical and preclinical Alzheimer disease. Alzheimer Dis Assoc Disord 2006;20(4):224–31.

Ashburner J, Hutton C, Frackowiak RSJ, Johnsrude I, Price C, Friston KJ. Identifying global anatomical differences: deformation-based morphometry. Hum Brain Mapp 1998;6:348–57.

Ashburner J, Friston KJ. Voxel-based morphometry – the methods. NeuroImage 2000;11:805–21.

Ashburner J, Friston KJ. Why voxel-based morphometry should be used. NeuroImage 2001;14:1238–43.

Ashburner J, Csernansky JG, Davatzikos C, Fox NC, Frisoni GB. Thompson PM computer-assisted imaging to assess brain structure in healthy and diseased patients. Lancet Neurol 2003;2:79–88.

Bedell BJ, Narayana PA. Volumetric analysis of white matter, grey matter, and CSF using fractional volume analysis. Magn Reson Med 1998;39:961–9.

Bookstein FL. Principal warps: thin-plate splines and the decomposition of deformations. IEEE Trans Pattern Anal Mach Intell 1989;11:567–85.

Bookstein FL. Landmark methods for forms without landmarks: morphometrics of group differences in outline shape. Med Image Anal 1997;1:225–43.

Bookstein FL. Voxel-based morphometry should not be used with imperfectly registered images. NeuroImage 2001;14:1454–62.

Davatzikos C. Why voxel-based morphometric analysis should be used with great caution when characterizing group differences. NeuroImage 2004;23:17–20.

Duchesne S, Caroli A, Geroldi C, Frisoni GB, Collins DL. Predicting clinical variable from MRI features: application to MMSE in MCI. Med Image Comput Comput Assist Interv 2005;1:392–9.

Duchesne S, Caroli A, Geroldi C, Barillot C, Frisoni GB, Collins DL. MRI-based automated computer classification of probable AD versus normal controls. IEEE Trans Med Imaging 2008;27(4):509–20.

Friston KJ, Ashburner J. Generative and recognition model for neuroanatomy. NeuroImage 2004;23:21–4.

Gashler M, Ventura D, Martinze T. Iterative non-linear dimensionality reduction with manifold sculpting.Advances in neural information processing systems, vol. 20; 2008. p. 513–20.

Grenander U, Miller MI. Computational anatomy. Q Appl Math 1998;4:617–94.

Hill DLG, Batchelor PG, Holden M, Hawkes DJ. Medical image registration. Phys Med Biol 2001;46:r1–45.

Lafon S. Diffusion maps and geometric harmonics. PhD thesis, Yale Univ.; 2004.

Meyer C, Boes J, Bland P, Zasandy K, Kison P, Koral K, et al. Demonstration of accuracy and clinical versatility of mutual information for automatic multimodality image fusion using affine and thin plate spline warped geometric deformations. Med Image Anal 1997;3:195–206.

Molloy DW, Standish TI. A guide to the standardized min-mental state examination. Int Psychogeriatr 1997;S1:87–94.

Pluim JPW, Maintz JBA, Viergever MA. Mutual information based registration of medical images: a survey. IEEE Trans Med Imaging 2003;22(8):986–1004.

Schölkopf B, Smola A, Muller K-R. Kernel principal component analysis. Lect Notes Comput Sci 1997;1327:583–8.

Thompson PM, Toga AW. Brain warping. Academic Press; 1999. p. 311–36.

Torgerson WS. Multidimensional scaling: I. Theory and method. Psychometrika 1952;17:401–9.

Roweis ST, Saul LK. Nonlinear dimensionality reduction by locally linear embedding. Science 2000;290:2323–6.

Venna J, Kaski S. Local multidimensional scaling. Neural Netw 2006;19:889–99.

Woolrich MW, Jbabdi S, Patenaude B, Chappell M, Makni S, Behrens T, et al. Bayesian analysis of neuroimaging data in FSL. NeuroImage 2009;45:S173–186.

Young FW, Hamer RM. Theory and application of multidimensional scaling. Eribaum Associates; 1994.